HEFAT2012
9th International Conference on Heat Transfer, Fluid Mechanics and Thermodynamics
16 – 18 July 2012
Malta

EFFECTS OF ACOUSTIC ACTUATION FREQUENCY AND NOZZLE GEOMETRY ON HEAT TRANSFER AND FLOW CHARACTERISTICS OF AN IMPINGING CONFINED WATER JET

Kor O.*, Malak S. Özkol Ü.
*Author for correspondence
Department of Mechanical Engineering,
İzmir Institute of Technology,
Urla, İzmir,
Turkey,
E-mail: orcunkor@iyte.edu.tr

ABSTRACT

An experimental study is performed to investigate the effects of acoustic actuation on heat transfer and flow characteristics of an impinging confined water jet. The water, collected in a reservoir, is accelerated by means of free fall and impinged on a smooth plate at which constant heat flux is applied. Two different nozzle geometries were investigated: sudden and smooth contracting nozzle. The flow is actuated with a loudspeaker at different Strouhal numbers in the range of 0~1, where nozzle-to-plate spacing of 6 nozzle diameters are tested while Reynolds number is kept constant at 10000 to study the effects of other parameters.. Flow visualization, turbulence, and surface heat transfer measurements are performed in the scope of this work. A sharp, continuous and significant roll-up evidence is seen in the smooth contracting nozzle, with the actuation frequency of St=0.175, at the axial location of about z/D~2 where the acoustic actuation has caused a decrease in heat transfer. It is observed that turbulence measurements with hot film anemometry are also in consistency with the surface heat transfer measurements. Acoustic actuation is found to be ineffective both in generating new flow structures or enhancing heat transfer in the sudden contracting nozzle.

INTRODUCTION

Jet impingement is a widely used technique where higher rates of heat or mass transfer are required. A single liquid or gas jet impinging normally on a surface may be used to achieve enhanced coefficients for convective heating, cooling or drying. It is widely used in industrial applications such as annealing of metals, cooling of gas turbine blades, cooling in grinding process, tempering of glass plate, drying of textile and paper products. Especially, for electronic components which need highly efficient heat removals, jet impingement cooling offers suitable solutions. Numerous studies about single or multiple impinging jets on flat plates have been performed in recent years; nevertheless, there are still questions to be answered especially about the effects of different type of actuations on heat transfer and flow characteristics.

NOMENCLATURE

A	[m^2]	Area of the heated plate
D	[m]	Nozzle exit diameter
f	[Hz]	Actuation frequency
h	[W/m^2K]	Convective heat transfer coefficient
V	[m/s]	Nozzle exit velocity
$\overline{V}$	[m/s]	Mean velocity
v'	[m/s]	Fluctuating velocity
k	[W/mK]	Conductive heat transfer coefficient
$Nu = \frac{hD}{k}$	[-]	Nusselt number
$\mathrm{Re} = \frac{VD}{\nu}$	[-]	Reynolds number
$St = \frac{fD}{V}$	[-]	Strouhal number
Tu	[-]	Turbulence intensity
Q_A	[W]	Heat transfer in axial direction
Q_R	[W]	Heat transfer in radial direction
u	[-]	Uncertainty
x	[m]	Radial distance from nozzle exit
z	[m]	Axial distance from nozzle exit
Z	[-]	Nozzle-to-plate distance
q''	[W/m^2]	Total heat flux
Special characters		
ν	[m^2/s]	Kinematic viscosity
Subscripts		
A		Axial
R		Radial

There are many parameters affecting heat transfer and flow characteristics of an impinging jet flow, such as Reynolds number, nozzle-to-plate spacing, the geometry of the nozzle and actuation magnitude and frequency to name a few.

Martin (1977) showed that at Re<1000 the flow field exhibits laminar flow properties, at Re>3000 the flow has turbulent features, and a transition regions occurs between these two regimes [1]. It is known that an artificial actuation changes the turbulence characteristics of the flow and therefore, resulting in a change in heat transfer. Gardon and Akfirat (1965) suggested that the increasing the level of turbulence causes an increment in the heat transfer rate [2]. Part of our aim in this study is in the same line with this finding which is to promote the turbulence by an acoustic actuation in jet shear layer to investigate it effects on the heat transfer.

Confinement is another important parameter that affects impinging jet flow heat transfer characteristics. Obot et al. (1982) showed that confinement causes a reduction in the heat transfer rate [3]. Baydar and Ozmen's (2005) studies focusing on the flow structure and heat transfer characteristics of submerged and confined jets suggest that the effect of confinement on flow structure is significant for nozzle-to-plate spacing up to 2 [4].

Nozzle geometry is another important factor which affects heat transfer performance of an impinging jet. Popiel and Boguslawski (1988) showed that the area mean heat transfer due to an impinging jet issuing from a contoured nozzle is less than that of a jet from a sharp-edged orifice. According to their studies, the effect of nozzle geometry on heat transfer is most significant in the region near the stagnation point [5]. Köseoğlu and Başkaya (2010) studied the effects of nozzle geometry on impinging jet heat transfer as well, noting that lower heat transfer rates were attained for higher aspect ratio jets in wall jet region especially at small jet to plate distances, where aspect ratios of the jets were defined as the ratio of major axis length to minor axis length [6].

Hwang et al. (2003) studied on the effects of acoustic actuation on impinging jet's heat transfer. Their experiments showed that as the jet flow is acoustically actuated by St=1.2, the heat transfer rates are enhanced a little at the small nozzle-to-plate spacing because of the high turbulence intensity at the nozzle exit. They also suggested that, for the acoustic actuation of St=2.4, the heat transfer rates are reduced a little for small nozzle-to-plate spacing and the formation of the secondary peak of the heat transfer coefficients is delayed due to the low turbulence intensity of the jet core flow [7].

Zhou et al. (2004) have actuated the jet by positioning a mesh screen upstream of a jet impingement setup. They showed that heat transfer increases moderately up to Z/D=4, pointing out that this enhancement is attributed to the increased turbulence within the potential core [8].

Bhattacharya et al. (2010) have focused on a more direct actuation method. They placed a stationary cylinder, an eccentrically mounted cylinder and an airfoil in the downstream of an impinging jet, letting it rotate around a pin which is fixed to the assembly. The ensuing oscillating jet configurations showed higher heat transfer rates than non-actuated jet tested under the similar conditions. The improved heat transfer characteristics were attributed to two mechanisms consisting of enhanced mixing/turbulence due to bluff body wakes vortex dynamics and oscillatory dislocation of the stagnation streamline [9].

EXPERIMENTAL SETUP

Figure 1 illustrates the schematic view of our experimental setup. The fluid in the supply tank is elevated to the reservoir mounted on a higher level, where the water free surface is kept at constant level. Water, which is accelerated with free fall, is passed through a honeycomb that is located in the pipe between the water tank and the jet room, and impinged to the flat plate with a mean velocity of 2 m/s, corresponding to the Reynolds number of 10000. The jet room is not only confined by the plane which coincides with the jet, but also from side walls as shown in Figure 1. Acoustic actuation signal is generated by means of an amplifier and then fed to the loudspeaker of which generates the acoustic waves. The loudspeaker is mounted on the top of the reservoir; hence, the waves are applied perpendicularly to the water surface. Strouhal number, which is the dimensionless form of actuation frequency, is adjusted by tuning the frequency. Other parameters governing Strouhal number, such as jet inlet velocity and nozzle diameter are kept constant at each experiment. The waveform and frequency of acoustic waves are adjusted via a function generator. The water is then sent back to the supply tank (in heat transfer and turbulence measurements experiments), or drained as waste (in flow visualization experiments).

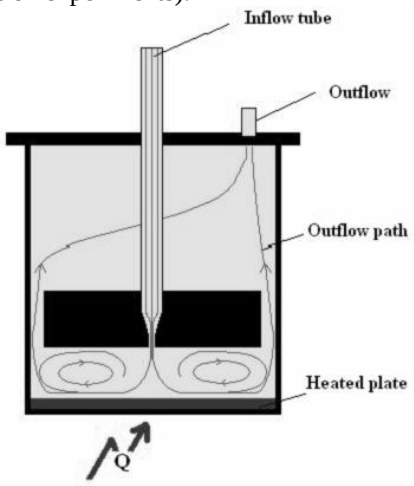

Figure 1 Schematic view of the test section

The copper flat plate, whose conductivity is about 390 W/mK, with an area of 400 cm^2 is heated by a wire resistance, whose power is approximately 1020 W. This corresponds to a uniform heat flux of $q'' = Q_{net} / A_{plate} = 2.55\ \mathrm{W/cm^2}$. The bottom part of the heating resistance is insulated with a cork plate insulator, to guard the heat losses and each side of wire is coated with thermal-conductive cement, for the purpose of minimizing contact resistance effects. The flat plate has a thickness of 5 mm to provide a uniform heat flux in axial direction. Radial uniformity is also satisfied which can be mathematically shown in equation (1). The radial heat transfer on the flat plate adjacent data points are calculated and the non-

uniformity in radial direction is found to be insignificant, which can be seen in Figure 4.

Temperature measurements are performed in radial direction, starting from the stagnation point of the impinging jet, with a sampling frequency of 0.5 Hz which corresponds St=0,00125. The temperature data is acquired by means of extra pure grade 34AWG J-type thermocouples located with a spacing of 2 mm in the vicinity of stagnation point. 12 thermocouples were used at the radial locations x/D=0, 0.5, 1, 1.5, 2.5, 3, 3.5, 4, 4.5, 7, 10 and 15. Inlet water temperature is also measured. The distance between each thermocouple head and the wet surface is kept at 1 mm so that, no significant temperature gradient between them would occur. Collected data is used in the calculation of convective heat transfer coefficient and therefore Nusselt number at each point as follows:

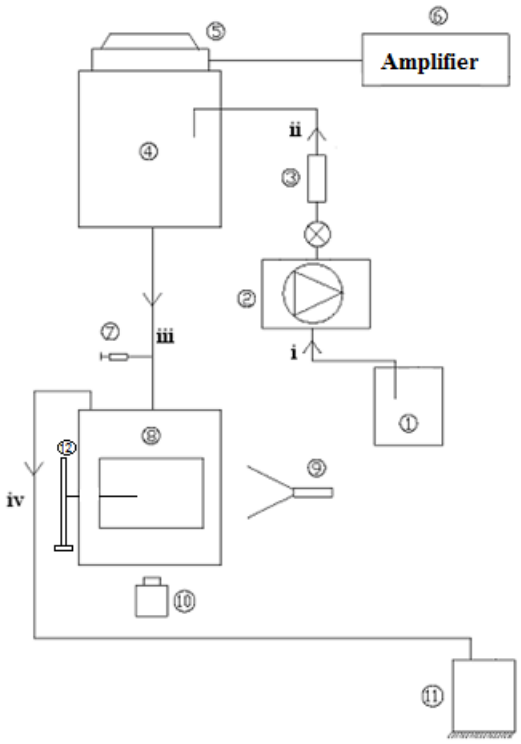

1. Supply Tank

2. Pump

3. Flow meter

4. Water tank

5. Loudspeaker

6. Amplifier and cold plate

7. Red food-dye Injection

8. Jet room

9. Laser

10. Charge Coupled Device (CCD) camera

11. Drainage

12. Hot-wire traverse mechanism

i. Supplying pump line

ii. Supplying water tank line

iii. Jet supplying system line (in)

iv. Jet supplying system line (out)

Figure 2 Experimental setup for water jet

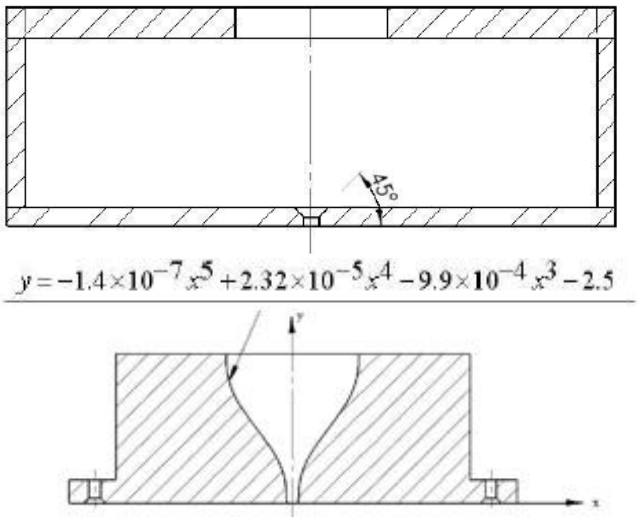

Figure 3 Investigated nozzle geometries; sudden or sharp contraction on top, smooth nozzle on bottom

$$Q_R = -kA_{cr}\left.\frac{dT}{dx}\right|_{x_1}^{x_2} = -k2\pi rH\left.\frac{dT}{dx}\right|_{x_1}^{x_2} \quad (1)$$

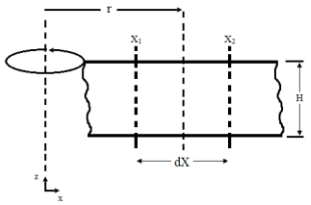

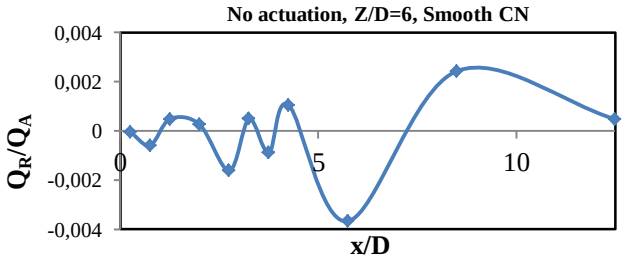

Figure 4 Calculation method of equation (1) on top and the ratio of radial to axial heat flows on the bottom

$$h = \frac{Q_{net}}{A_{plate}(T_{x/D} - T_{inlet})} \quad (2)$$

$$Nu = \frac{hD_{jet}}{k_w} \quad (3)$$

The uncertainty of each measured value is calculated with the confidence limit of 95%, by the method suggested by Kline et al. (1953) [10]. The uncertainty in Reynolds and Nusselt numbers are found to be ±3.6% and 1.9% respectively.

Flow visualization experiments are also performed in the scope of this work. A CCD camera is used for capturing images of the jet flow where the cross-section of the jet is illuminated by means of a green laser sheet with a wavelength of 532 nm. Red food dye (Rhodamine B) is used as the marking fluid. Experiments are ended when the dye clouded the test section such that it becomes impossible to distinguish the turbulent structures anymore. Though it's impossible to obtain any velocity measurement data from these images, a clear understanding on how the flow structures are affected from acoustic actuation can be derived easily. Besides, the instantaneous images captured in a certain period are ensemble averaged to obtain the dominant flow characteristics at a given case. Ensemble averaging is done by averaging the pixel information of 100 images which corresponds to the same physical location in space.

Turbulence measurement experiments are conducted using a TSI 1276-10AW model hot film sensor attached to the TSI IFA-300 model constant temperature anemometer. Hot film sensor has dimensions which 0.25mm in active length and 0.0254mm in diameter. . The data is acquired at 10 kHz sample rate and for approximately 6.55 seconds. The range of measurements are performed in the radial direction ranging from the jet centreline (x/D=0) to 2.4D for jet profile data and to 8.5D for near wall data. Wall normal measurement locations are at z/D=5.8, 5, 4, 3, 2, 1, 0.2 for jet profile data and at z/D=0.2 for near wall data. The distance between data points is 0.1D.

RESULTS AND DISCUSSION

Flow Visualization

Flow visualization experiments are performed for Strouhal numbers of 0.125, 0.175, 0.25, 0.5, 0.7 and 1 for both smooth and sudden contracting nozzle geometries. Nozzle-to-plate spacing is kept at the level of Z/D=6.

Compared with the no acoustic actuation case, it can be suggested that Strouhal number (St) has a spreading effect on jet flow. Especially for St=0.175, the effect of acoustic actuation on flow structures becomes more significant, where a sharp and a steady roll-up effect is seen at z/D=2, as this effect leads to a spreading on the jet shear layer. The roll-up structures can be seen in the instantaneous images listed in Figure 5, as well as in the ensemble averaged images presented in the same figure. Although the flow structures responds to actuation at any level, the case of St=0.175 exhibits the most significant response. An axisymmetric, consistent and continuous roll-up causes the jet to get slightly narrower downstream of the roll-up. Our experiments show that, the roll-up event is first introduced at the actuation level of St=0.125, which is not as significant as St=0.175. For St=0.25, a similar but much weaker effect is seen as well. Actuation frequency corresponding to St=0.5 results in a roll-up event of which is sharper than the one of St=0.25, but weaker than St=0.175. From this point on, increasing Strouhal number makes diminishing effect on roll-up event, up to St=1, where at this actuation level, no roll-up is seen and the jet gets as narrow as its non-actuated situation.

In contrast to smooth contracting nozzle, the application of acoustic actuation on jet flow through a sudden contracting nozzle results in a quite different flow. As it can be seen from Figure 5.b, the roll-up occurrence is not seen in the sudden contracting nozzle. It is considered that, the nozzle geometry itself triggers the evolution of energetic turbulent structures that our actuation energy would not be able to overcome. These energetic turbulent scales are thought to dominate the structures created by acoustic actuation at any Strouhal number. Since no velocity measurement experiments are performed, the physical phenomenon lying behind this fact cannot be understood in a fluid mechanical way. Nevertheless, heat transfer measurements collected during these cases will be discussed below. Another point that should be noted is the difference in growth of shear layer for different nozzle geometries. The jet shear layer becomes turbulent at about z/D≈1 for smooth contracting nozzle; on the other hand it becomes turbulent as soon as it comes out sudden contracting nozzle, as seen in Figure 6.b. The immediately starting turbulent shear layer is thought to be due to the fact that the flow makes much tighter turns in this nozzle configuration, which results in much higher pressure gradients. These sharp gradients result in much finer turbulent scales. However, these considerations are suggested by commenting on the visualization images, not on measurements. Further experimental measurements should be performed for a more accurate reasoning.

Effect of Actuation on Heat Transfer

The effect of acoustic actuation on heat transfer for given Strouhal numbers is not found to be significant in a positive way. Figure 7 shows normalized Nusselt number distributions in radial direction. It can be seen that the acoustic actuation in the range of $0 < St \leq 1$ results in decrease of Nu number in general. Nu number decreases with decreasing Strouhal number, where St=1 results in the highest Nu number next to no actuation case. The most striking feature seen from the Figure 7 is that the effect of the acoustic actuation is most significant in the stagnation region. The difference between the Nusselt numbers diminishes with increasing radial distance. There is almost no difference in Nusselt numbers beyond x/D=5. Which is to say that our acoustic perturbation has no effect beyond x/D=5. The distribution of Nu number shows that, beyond the maximum at the stagnation point, heat transfer coefficient decreases in the radial direction up to x/D=1. This minimum is followed by another peak at x/D=2.5, and then another decrease. Nusselt number makes a plateau between $3 < x/D < 4.5$. Beyond x/D=4.5, Nusselt number decreases up to x/D=7 and with a slight increase plateaus beyond that.

Similarly, normalized Nusselt number curves are plotted in Figure 8 for different nozzle geometries. It can be seen here that for non-actuated jets, smooth contracting nozzle provides higher heat transfer coefficient in the stagnation region in comparison with sudden contracting nozzle. On the other hand, these profiles seem almost independent from nozzle geometry especially for the radial locations closer to the jet centre-line, except at two individual points which are thought to be experimental outliers, for actuated cases. These findings lead us to suggest that the wall-jet shear layer independently grows of from the nozzle geometry both for actuated and non-actuated jet flows. The distribution of Nu number with respect to axial distance x/D for different cases show us again that, maximum (x/D=0, 2.5, 3.5, 4.5) and minimum (x/D=1, 3, 4, 7) peaks occur nearly at the same locations, consistently. It is observed that the sudden contracting nozzle results in clearly higher heat transfer coefficients at the stagnation region for St=0.175, however; in the outer boundaries of the wall jet, smooth contracting nozzle gives higher heat transfer.

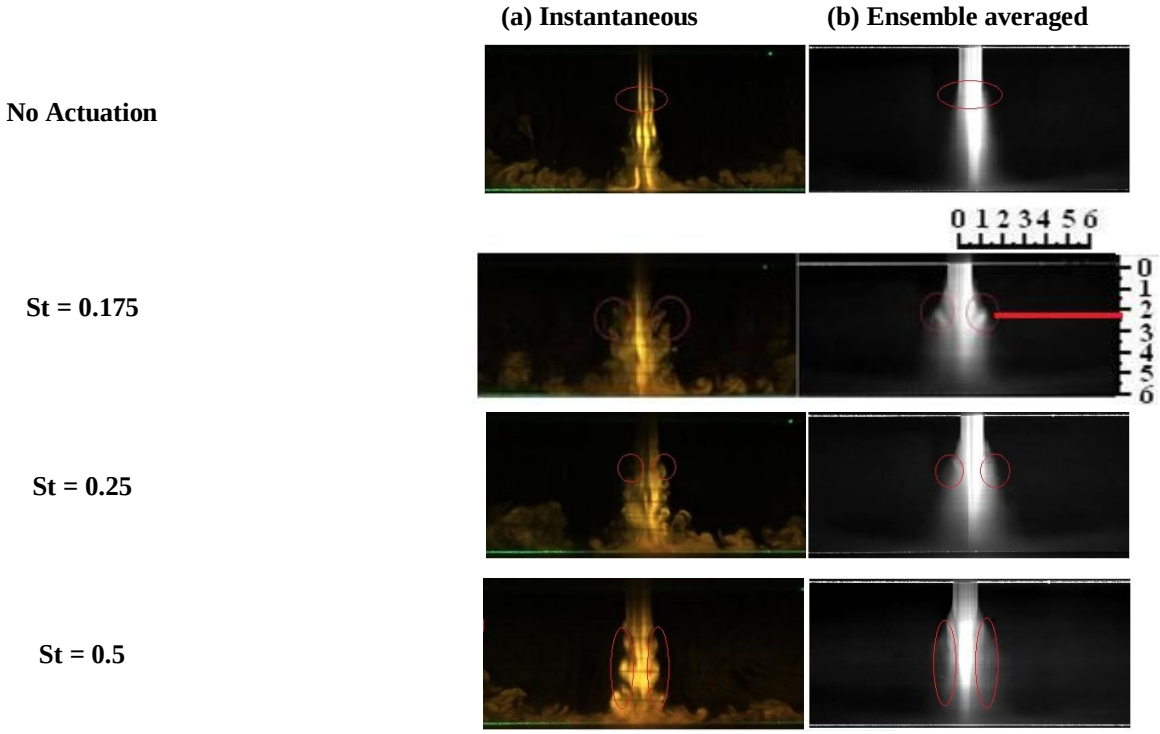

Figure 5 Instantaneous vs. ensemble averaged images, Smooth contracting nozzle

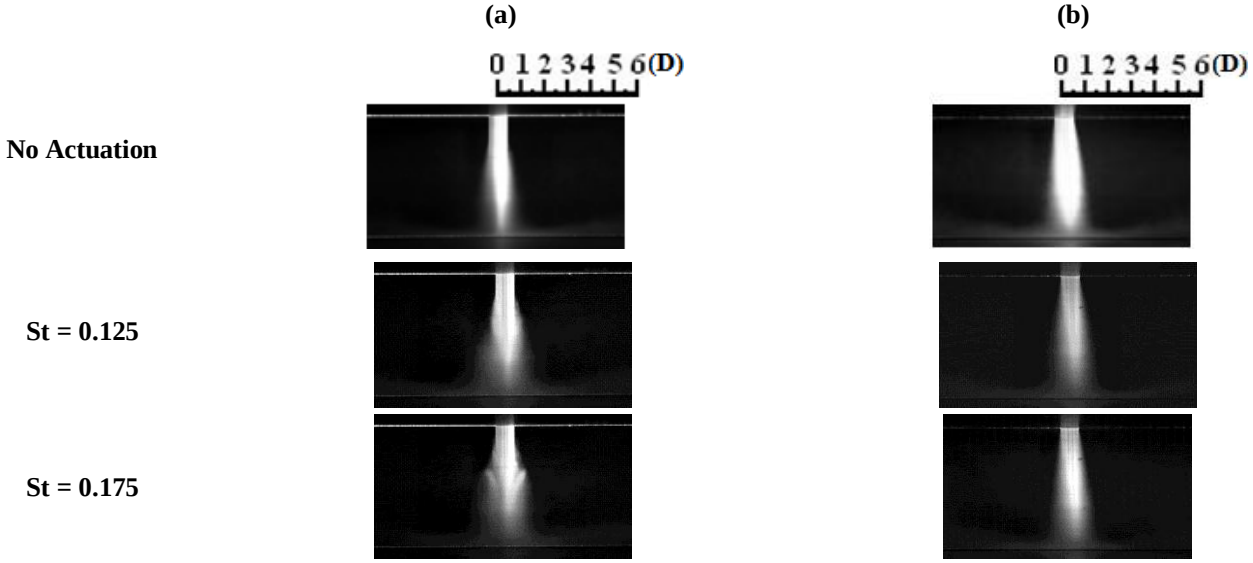

Figure 6 Ensemble averaged images (a) Smooth cont. nozzle (b) Sudden cont. nozzle.

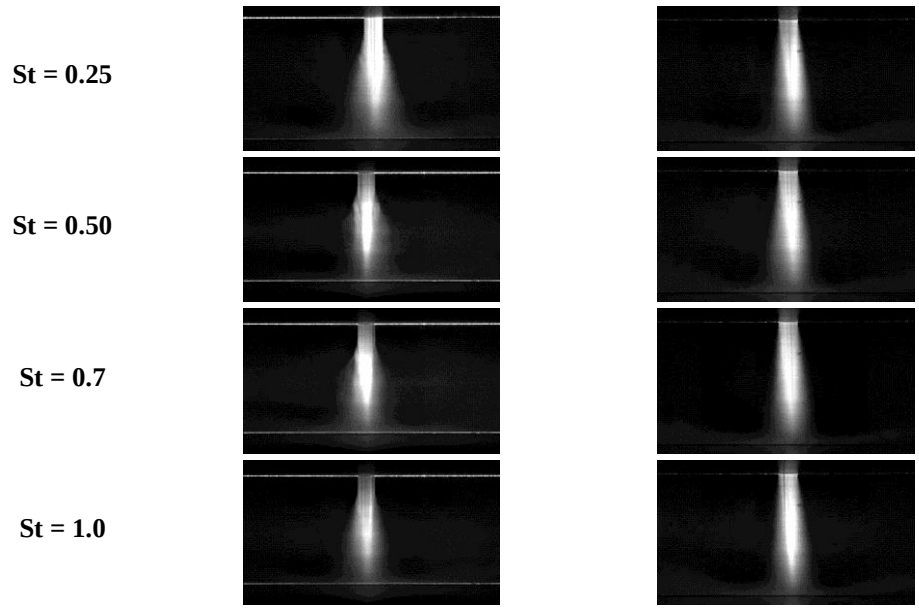

Figure 6 – cont.

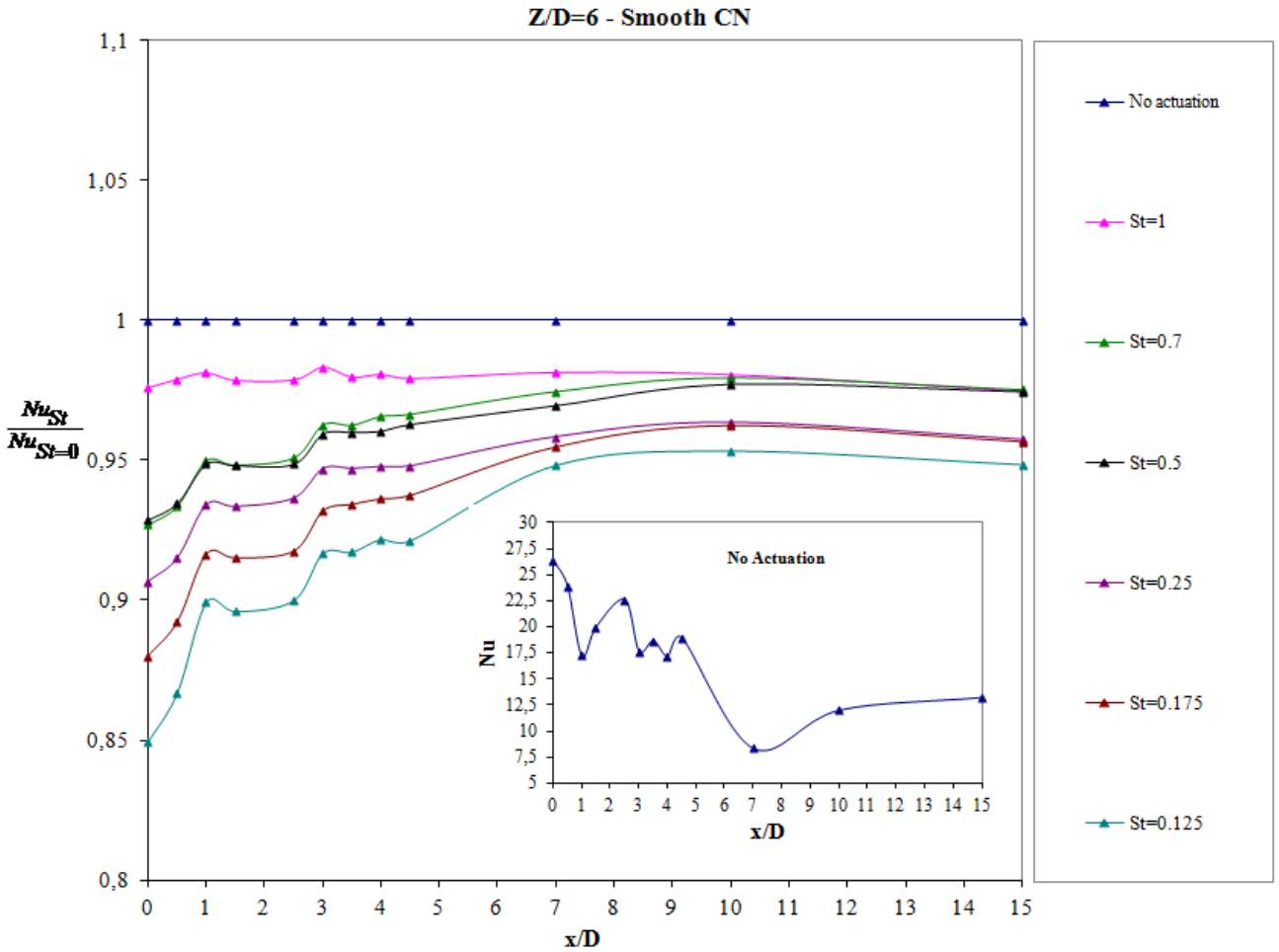

Figure 7 Nusselt number distribution on the hot plate. (Small figure inside the graph is the exact Nu distribution of non-actuated case)

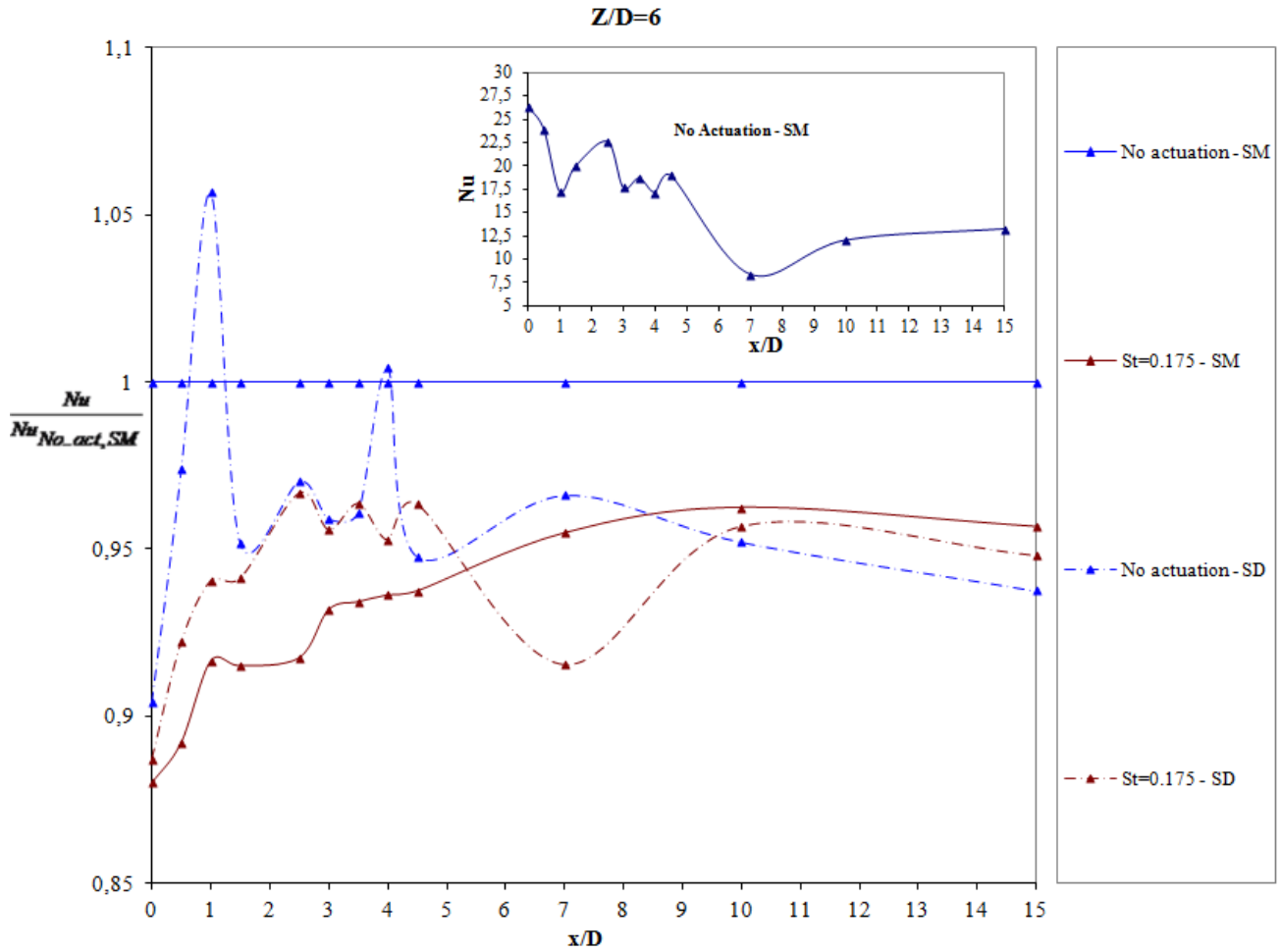

Figure 8 Nusselt number distribution on the hot plate for different nozzle geometries. (Small figure inside the graph is the exact Nu distribution of non-actuated case). SM: Smooth Nozzle, SD: Suddenly Contracting Nozzle

Turbulence Intensity Measurements

Hot film senses heat transfer from the wire to the fluid. Anthoine et al. state that the velocity data acquired by the hot film is directionally ambiguous since the probe is single; hence, the cooling velocity sensed by the hot film gives the effective cooling velocity referring to all directions [11]. However, once the measurements are performed in the jet core region, the output is thought to represent only the velocity in axial direction, where the velocity component in radial direction is negligible with respect to axial velocity. In contrast, in the wall jet region, the radial velocity becomes more dominant and the velocity sensed by the hot film represents the radial velocity. It should be noted that, for the remaining parts of the flow, the data is directionally ambiguous and refers to the resultant of radial and axial values.

Turbulence intensity calculations are conducted with this manner. The simple formulation giving the turbulence intensity can be seen in equation (4):

$$Tu = \frac{\sqrt{\overline{v'^2}}}{\overline{V}} \times 100 \qquad (4)$$

Turbulence measurements were performed for one Reynolds number (10000) and three different Strouhal numbers (0, 0.175 and 1). For three different actuation cases, radial distribution of Nusselt number and turbulence intensity are plotted in Figure 9. An interesting formation was observed when these plots were examined. The turbulence intensity maximums at locations of x/D~0.5 and x/D~2.5 have a mixed effect on Nusselt number. In the high turbulence region near to the stagnation point, Nusselt number was also high, for all Strouhal values. However, Nusselt number was continuously measured low in the high turbulence level region at x/D~2.5, which is an unexpected formation. A sharp drop on turbulence intensity has been observed at x/D=2.5. It is thought that, the reason of this drop is a change on flow regime (turbulent flow →transient flow) due to characteristic of flow. The flow visualization studies show that semi periodic vortex structures exist in wall jet zone about the radial location of x/D~2.5. It is thought that these vortex structures circulate the hot fluid and eventually cause it to interact with the thermal boundary layer of wall. This interaction results in a negative effect on cooling of the wall at this location, although the turbulence intensity is high.

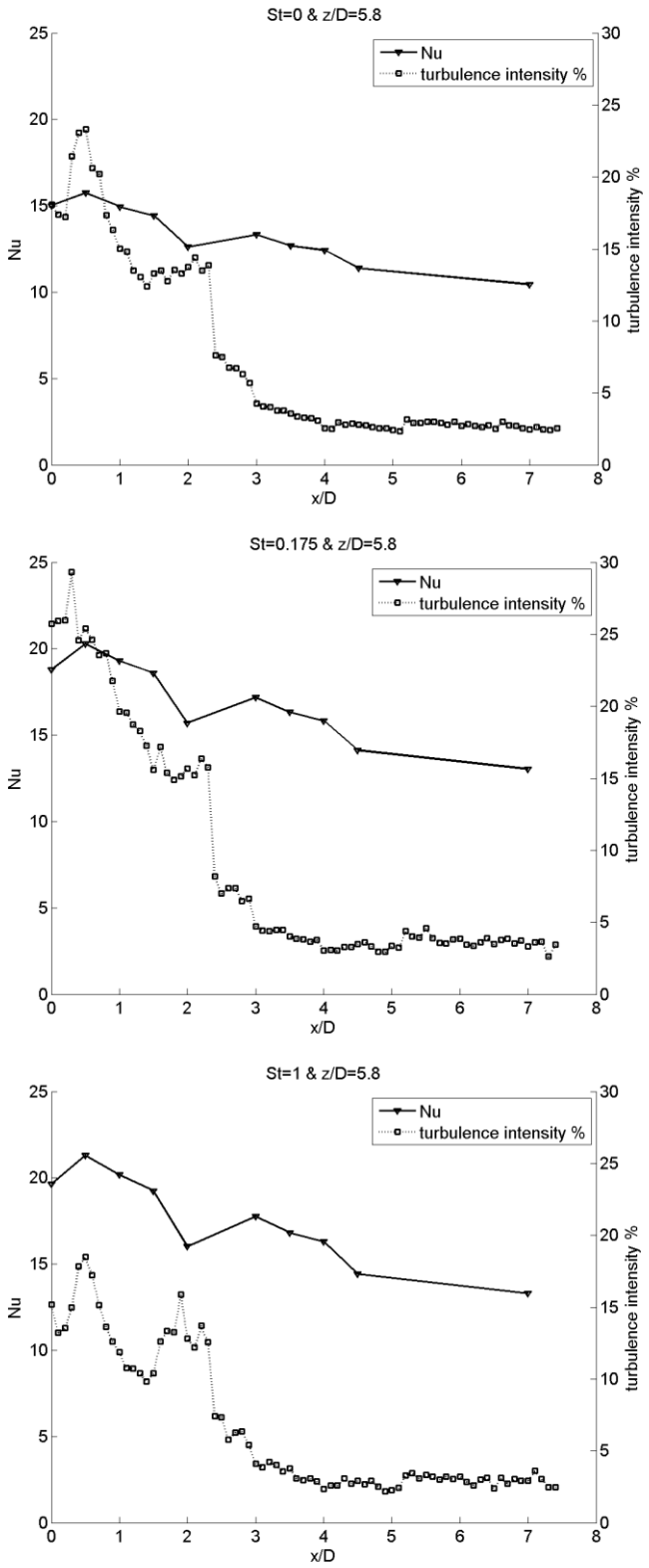

Figure 9 Radial distribution of Nusselt number and turbulence

CONCLUSIONS

Flow visualization, heat transfer and turbulence measurement experiments of an acoustically actuated round, submerged and confined jet are performed in the scope of this work. Reynolds number is kept at around 10000 for all experiments. Dimensionless nozzle-to-plate spacing, Z/D, is kept at 6. Strouhal number, is changed in the range of $0 < St \leq 1$. Two nozzle geometries are used during experiments are smooth and sudden contracting nozzles.

Strouhal number is found to be effective especially on flow structures observed in smooth contracting nozzle. For nozzle-to-plate spacing of 6 nozzle diameters, with the actuation frequency of St=0.175, a sharp, continuous and significant roll-up event is seen at the axial location of about z/D~2, which eventually results in a spread of the jet significantly. Roll-up effect loses its sharpness (coherence in the visualization experiments) for St=0.25. Another roll-up event which is not as significant as St=0.175 is seen again for St=0.5. For Strouhal numbers between 0.5 and 1, roll-up diminishes and loses its character totally for St=1. The acoustic actuation has caused a decrease in heat transfer for Z/D=6. Turbulence measurements show that, although the turbulence intensity level is high, expected heat removal does not occur which means recirculation of fluid in the jet room has a decreasing effect on heat transfer at about the radial location of x/D~2.5.

Transition to turbulence in the shear layer of the jet is obtained at z/D≈1 for smooth contracting nozzle. Nevertheless, no laminar region is observed for sudden contracting nozzle, as the shear layer in this case became turbulent immediately. Nevertheless, these differences in flow properties do not make significant effect on the Nusselt number distribution.

It must be noted that, in contrast with the most of the studies found in literature, impinging jet region is confined not only by the walls at both sides, but also by the top plane in the present study. It is thought that, this situation has caused the coolant circulate in the jet room. Hence, while some of the coolant is moved away from the test section immediately, a considerable amount of heated coolant is kept in the jet room which result in a considerably decreased Nu number. This phenomenon is thought to be the reason of lowered and uncommon distribution of Nusselt number in our studies.

ACKNOWLEDGEMENTS

This work was supported by The Scientific and Technological Research Council of Turkey (TÜBİTAK), and İzmir Institute of Technology.

REFERENCES

[1] Martin, H., 1977. Heat and mass transfer between impinging gas jets and solid surfaces. *J. Matter. Process. Technol.*, Vol.136, 1-3, pp 1-60

[2] Gardon, R., Akfirat, J. C. 1965. The role of turbulence in determining the heat transfer characteristics of impinging jets. *Int. J. Heat and Mass Transfer*, Vol.8, pp.1261-1272

[3] Obot, N.Y., Mujumdar, A.S, Douglas W.J.M. 1982. Effect of semi-confinement on impingement heat transfer, *Proc. 7th Int. Heat Transfer Conference*, Germany, Vol.3, pp.395-400

[4] Baydar, E., Ozmen, Y. 2006. An experimental investigation on flow structures of confined and unconfined impinging air jets, *Heat and Mass Transfer*, Vol.42, pp.338-346

[5] Popiel, C.O., Boguslawski, L. 1988. Effect of flow structure on the heat or mass transfer on a flat plate in impinging round jet, *UK National Conference on Heat Transfer*, Vol.1, pp.663-685

[6] Köseoğlu, M.F., Başkaya, S. 2010. The role of jet inlet geometry in impinging jet heat transfer, modeling and experiments. International *Journal of Thermal Sciences*, Vol.49, pp 1417-1426

[7] Hwang, S.D., Cho, H.H. 2003. Effects of acoustic excitation positions on heat transfer and flow in axisymmetric impinging jet: main jet excitation and shear layer excitation, *Int. Journal of Heat and Fluid Flow*, Vol.24, pp.199-209

[8] Zhou, D.W. and Lee, S.J. 2004. Heat transfer enhancement of impinging jets using mesh screens. *Int. Journal of Heat and Mass Transfer*, Vol 47, pp.2097-2108

[9] Bhattacharya, S., Ahmed, A. 2010, A note on unsteady impinging jet heat transfer, *Experimental Thermal and Fluid Science*, Vol. 34, pp.633-637

[10] Kline, S.J., McClintock, F.A. 1953. Describing uncertainties in single sample experiments, Mechanical Engineering, Vol.75, pp.3-9

[11] Anthoine J., Arts T., Boerrigter H.L., Buchlin J. M., Carbonaro M., Degrez G., Dénos R., Fletcher D., Olivari D., Riethmuller M.L., Van den Braembussche R.A., (2009), Measurement techniques in fluid dynamics , *An Introduction. Von Karman Institute for Fluid Dynamics.*